Performance Improvement of Monte Carlo Localization in Outdoor Environment Using Modified Sensor Model with Standard Elevation Map

Tae-Bum Kwon, Jae-Bok Song and Sang-Hyun Joo

Abstract—**Mobile robot localization in outdoor environments is a main issue of this paper. In this paper, MCL with a laser scanner uses a reference elevation map to estimate a robot pose. The MCL shows low performance when it uses an elevation map because an elevation map cannot represent the environment in detail. Therefore, other types of maps have been proposed to improve the localization performance. An elevation map, however, should be used as the main reference map in some applications, so we modified the sensor model for MCL to improve its localization performance when it does use an elevation map. A new probability distribution, which considers the discrepancy between the elevation map and the real environment, is added into the conventional sensor model. The real experiments that were performed in the outdoor environment indicated that the modified sensor model proposed in this research was able to improve the localization performance of MCL. Therefore, the proposed modified sensor model is considered very useful when an elevation map is used as the reference map.**

I. Introduction

Localization is one of the most important techniques in mobile robot navigation in both indoor and outdoor environments. Various types of maps, such as a grid map, elevation map, topological map, and so on, can be used for localization [1]-[4]. A 2-D grid map is an efficient and sufficient map when a robot with a range sensor navigates in the indoor environment because the ground is flat and the range sensor measures the distance to the object at a fixed height. In such a case, the motion of the robot can be expressed as 3 DOF motion (x, y, θ) in 2-D space. However, when a robot navigates in the outdoor environment, 6 DOF motion (x, y, z, roll ψ, pitch θ, yaw φ) in 3-D space needs to be estimated, so the environment needs to be represented by a 3-D map for localization.

An elevation map is the most popular map for representing a 3-D outdoor environment [5], [6]. In this map, the environment is regularly divided into small cells (e.g., 0.1m*0.1m), and each cell has its own elevation information. An accurate elevation map can be generated for localization by using the aerial mapping system equipped with both a GPS/INS for localization and a lidar sensor for range data acquisition. This type of map is suitable for large outdoor environments and is used as the main map for special applications such as military vehicles [7].

If GPS/DGPS data are available, the localization problem in the outdoor environment can be practically solved to some extent. Therefore, little research has been done on outdoor localization with respect to a pre-given reference map, whereas much research has been done on environment modeling based on the SLAM technique [8]-[11]. However, the GPS/DGPS-based localization schemes cannot be successfully used for some applications such as military robots, which may be exposed to anti-GPS signals. In this case, the given elevation map becomes the only reference data, so the data obtained from the sensors mounted on the robot are matched with this reference data for localization.

Localization techniques such as the Kalman filter-based localization, Markov localization, Monte Carlo localization (MCL), and so on estimate a robot pose with respect to a reference map [12]-[17]. Among them, MCL has been most widely used because of its many advantages, and its high performance in indoor environments has been recently demonstrated. In recent years, MCL has been applied to outdoor localization problems. This study also used MCL to estimate a robot pose in the outdoor environment. However, its performance such as the success rate of global localization was generally lower than that of indoor localization.

This study used an elevation map, which was given in advance, to investigate ways to improve the performance of MCL in the outdoor environment. Although a new type of map was proposed to improve the performance of MCL in the outdoor environment [3], [4], a standard elevation map should be used as the main map in some applications. Therefore, the performance improvement of MCL with a standard elevation map is valuable. Furthermore, we present a new sensor model and evaluate how localization performance can be improved with the new sensor model, instead of the conventional sensor model.

This paper is organized as follows. Related work is discussed in section 2, and MCL is briefly reviewed in section 3. The discrepancy between an elevation map and real data from a range sensor such as a laser scanner is presented in

Authors are gratefully acknowledging the financial support by Agency for Defense Development and by UTRC (Unmanned Technology Research Center), Korea Advanced Institute of Science and Technology.

Tae-Bum Kwon is with the Korea University, Korea. (e-mail: haptics@korea.ac.kr).

Jae-Bok Song is with the Korea University, Korea. (corresponding author to provide phone: +82-2-3290-3363; fax: +82-2-3290-3757; e-mail: jbsong@korea.ac.kr).

Sang-Hyun Joo is with the Agency for Defense Development, Korea. (e-mail: jooshce@paran.com).

section 4. A modified sensor model for an elevation map is proposed in section 5, and the experimental results of outdoor localization are presented in section 6. Finally, conclusions are presented in section 7.

II. Related Work

City modeling using a digital surface map (DSM), which is one of several types of elevation maps, has been conducted in [18], [19]. DSM is used as a reference elevation map and a vehicle pose with respect to the DSM is estimated through the MCL method. The range data obtained by a laser scanner is compared with those predicted from the DSM to estimate a vehicle pose. This is an extension of 2-D MCL from an indoor environment to an outdoor environment. Whereas the path generated by the scan matching method becomes less accurate as a vehicle moves, the path generated by MCL is accurate without error accumulation even after a vehicle has traveled more than 10 km because it estimates a pose with respect to the reference map. However, this research did not deal with global localization through MCL but a vehicle pose was only locally tracked with a known initial pose. While it was shown that the error of local tracking did not increase unboundedly as the vehicle moved, the performance of localization was not analyzed quantitatively.

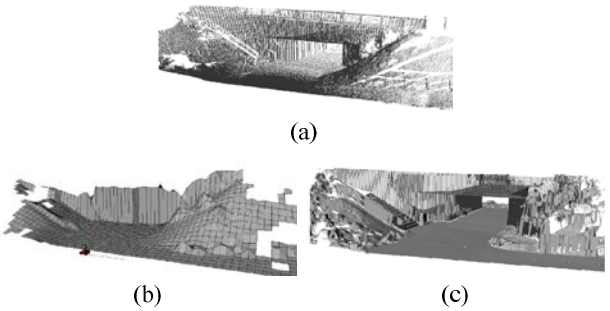

Fig. 1. Difference of map representation; (a) point clouds, (b) elevation map, and (c) multi-level surface map. (All figures are quoted in [4].)

Another similar research about outdoor localization was conducted in [3], [4]. In this study, a robot pose was estimated by the MCL method using an elevation map and the new type of map. To overcome the disadvantages of MCL with a standard elevation map, which were already mentioned, a multi-level surface map was proposed to improve the performance of MCL in the outdoor environment. The success rate of global localization and the accuracy of local tracking were empirically evaluated. The MCL performance with a multi-level surface map was better than that with a standard elevation map. Figure 1 in [4] shows the standard elevation map and the proposed multi-level surface map. A multi-level surface map in Fig.1(c) can describe the environment in detail, but building such a map is very complicated and difficult, whereas a standard elevation map such as DSM can be generated relatively easily. Furthermore, as mentioned in the introduction section, because an elevation map should be used as a reference map in some applications, the improvement of MCL performance with a standard elevation map needs to be investigated.

III. Monte Carlo Localization

Monte Carlo localization (MCL) is used for localization in this research. It is one of the popular Bayesian filters that can track the distribution of probability using a set of random samples. At each time step, the probabilities of samples are updated using a motion model and a sensor model, and then the samples are re-sampled. The state (a robot pose in this case) is represented by the weighted sum of all samples. This section reviews MCL very briefly. More details on MCL can be found in [17], [20]-[21].

A. Bayes Filtering

MCL represents a robot's positional certainty at an arbitrary location in a given grid map. The robot calculates the posterior probability $Bel(x_t)$ by using the Bayes filter based on odometry and range data as follows:

$$Bel(x_t) = p(x_t \mid z_{0:t}, u_{0:t}) \tag{1}$$

where x_t denotes the robot pose (x, y, θ) at time t, $z_{0:t} = \{z_0, z_1, \ldots, z_t\}$ denotes the measurements of the range sensors (e.g., laser scanner, sonar, IR sensor, etc.) up to t, and $u_{0:t} = \{u_0, u_1, \ldots, u_t\}$ is the odometric data from the wheel encoder. In order to cope with various uncertainties, the robot uses probability models to reflect the errors: sensor model (or perception model) and motion model (or action model). The Bayes filter can be finally represented by the following equation:

$$Bel(x_t) = \eta\, p(z_t \mid x_t) \int p(x_t \mid x_{t-1}, u_t)\, Bel(x_{t-1}) dx_{t-1} \tag{2}$$

where η is the normalizing constant, $p(x_t \mid x_{t-1}, u_t)$ is the motion model, and $p(z_t \mid x_t)$ is the sensor model.

B. Particle Filters

The particle filter used in MCL represents the posterior distribution $p(x_t \mid z_{0:t}, u_{0:t})$ by using a set of random samples. Among the several variants of the particle filter, the SIR (Sampling Importance Resampling) algorithm is adopted in this research [22], [23]. This algorithm is composed of the following three steps; sampling, importance weighting and resampling. In sampling, a new sample set X'_t is generated from the past sample set X_{t-1} distributed by $Bel(x_{t-1})$. In importance weighting, the importance factor $\omega_t^{(i)}$ is evaluated using the sensor model.

$$\omega_t^{(i)} = \eta\, p(z_t \mid x_t'^{(i)}) \tag{3}$$

where η is a normalization constant and $x_t'^{(i)}$ is an element of set X'_t. In resampling, a new sample set X_t is randomly chosen from X'_t according to the distribution defined by the

importance factor $\omega_t^{(i)}$.

$$X_t = \{x_t^{(j)} \mid j = 1 \cdots N\} \sim \{x_t'^{(i)}, \omega_t^{(i)}\} \tag{4}$$

The prior probability of each sample of the new sample set X_t at time t is initialized to $1/N$. Through the recursive computation of three steps, the samples converge to the pose with the highest probability.

IV. Discrepancy between Elevation Map and Real Sensor Data

Each cell of an elevation map has the highest elevation if more than two objects are located on the same cell with different height values. For example, if part A on the lower floor and part B on the upper floor are located on the same cell of the elevation map in Fig. 2(a), that cell has the elevation of part B and the information of part A cannot be restored from the elevation map in Fig. 2(b). However, the range sensor, SICK laser scanner in this experiment, may sense all parts of the environment like Fig. 2(c) as the roll and pitch angles of the robot and the tilt angle of the laser scanner change. A large discrepancy, therefore, might occur between the elevation map and the range sensor data in some parts of the environment.

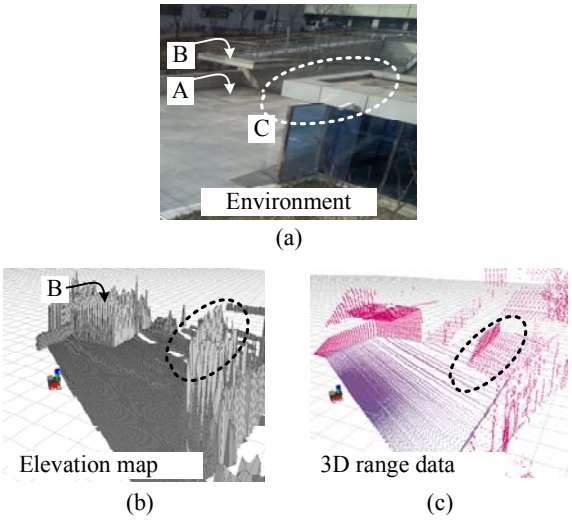

Fig. 2. Examples of discrepancy between elevation map and real range sensor data; (a) environment, (b) elevation map, and (c) real range sensor data.

Many environments with different shapes can be identically modeled into one elevation map. Figure 3 is an example, and the elevation map in Fig. 3(a) can represent all environments in Fig. 3(b)-(d). To perform MCL, range data should be predicted from the map, and in this case, the range is predicted as in Fig. 3(a), although the real environment is more complicated than those represented by the elevation maps in Fig. 3(b)-(d). This discrepancy deteriorates the accuracy of localization because MCL compares the range data obtained from the real environments such as Fig. 3(b)-(d) with those predicted from the map.

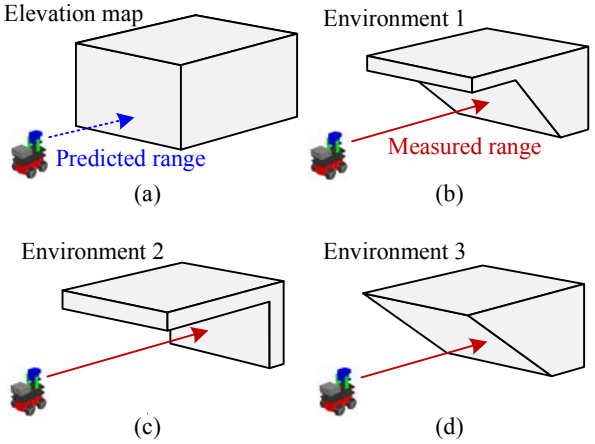

Fig. 3. Examples of environments to be modeled as an identical elevation map.

V. Modified Sensor Model

The range data of a sample predicted from the map are compared with the real sensor data in MCL, and the difference between the two data is transformed into the probability of that sample. This probability is calculated using a sensor model $p(z|x)$. The most important and popular sensor model for a laser scanner is given by ([3], [17], [20]-[21], [24]).

$$p(z \mid x) = \prod_{k=1}^{K} p(z^k \mid x) \tag{5}$$

where K is the number of sensing points, or beams, of one laser scan z. Note that the probabilities for all beams are multiplied because it is assumed that each beam is independent. The conventional sensor model $p(z^k|x)$, which is a sum of three different distributions, is given by

$$\begin{aligned} p(z^k \mid x) = {} & \alpha_{\text{obstacle}} \cdot p_{\text{obstacle}}(z^k \mid x) + \alpha_{\text{rand}} \cdot p_{\text{rand}}(z^k \mid x) \\ & + \alpha_{\text{max}} \cdot p_{\text{max}}(z^k \mid x) \end{aligned} \tag{6}$$

where $p_{\text{obstacle}}(z^k|x)$ calculates a probability based on the difference between the predicted range data and the sensor range data and is a Gaussian distribution with a variance σ^2. $p_{\text{rand}}(z^k|x)$ models the random measurements and is a uniform distribution from 0 to the maximum sensing range. $p_{\text{max}}(z^k|x)$ models the maximum range measurements using a point mass distribution. The three coefficients α_{obstacle}, α_{rand}, and α_{max} can be determined empirically. Fig. 4 shows one example of the conventional sensor model used in this research. This conventional sensor model may generate an unsuitable probability distribution, as shown in Fig. 5. In Fig. 5, the range predicted from the elevation map differs from the range sensor data, although the robot pose is accurate because the elevation map cannot model the environment in detail. Therefore, the probability calculated by the conventional sensor model, p_1 in

Fig. 5, is very low or zero, which mainly depends on $p_{\text{rand}}(z^k|x)$ in (6). It can cause samples to converge on an incorrect pose during global localization because the samples close to the true robot pose might be easily eliminated in the resampling steps of MCL.

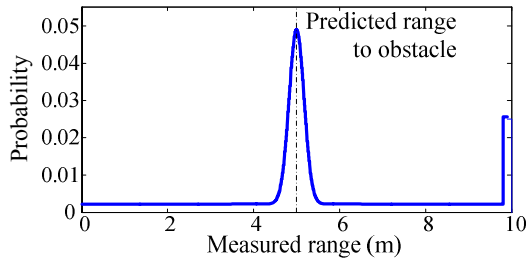

Fig. 4. Conventional sensor model for probability calculation based on difference between sensor data and predicted range data.

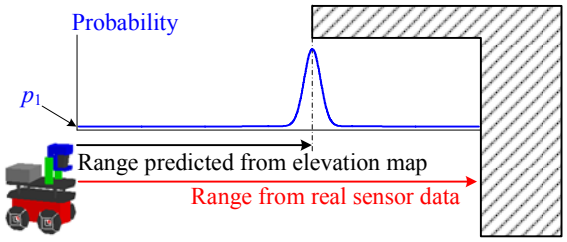

Fig. 5. Probability distribution by conventional sensor model with elevation map.

To reduce this unfavorably fast elimination of the samples close to the true robot pose, the sensor model should be modified. In this research, a new distribution which considers the discrepancy between the elevation map and the real environment is added into the conventional sensor model. As shown in Fig. 3, the discrepancy between the elevation map and the environment cannot be predicted because an infinite number of environments can be mapped into an identical elevation map. The discrepancy, therefore, is modeled by a uniform distribution beyond the obstacle position predicted from an elevation map. Then, the modified sensor model $p(z^k|x)$ can be represented as a sum of four different distributions as follows:

$$\begin{aligned} p(z^k \mid x) &= \alpha_{\text{obstacle}} \cdot p_{\text{obstacle}}(z^k \mid x) + \alpha_{\text{rand}} \cdot p_{\text{rand}}(z^k \mid x) \\ &\quad + \alpha_{\text{max}} \cdot p_{\text{max}}(z^k \mid x) + \alpha_{\text{discrepancy}} \cdot p_{\text{discrepancy}}(z^k \mid x) \end{aligned} \tag{7}$$

$$p_{\text{discrepancy}}(z^k \mid x) = \begin{cases} \dfrac{1}{b-a} & \text{for } z^k \in [a,b] \\ 0 & \text{otherwise} \end{cases} \tag{8}$$

where $p_{\text{discrepancy}}(z^k|x)$ is a uniform distribution from a to b, in which a means the point from which the uncertainty due to the discrepancy between the elevation map and the environment starts. In this research, a is defined as the predicted range to the obstacle plus 2σ, and b is the maximum sensing range. $\alpha_{\text{discrepancy}}$ is adjusted to make the function (or equation (7)) continuous, and the whole probability distribution of the modified sensor model is shown in Fig. 6. This modified sensor model may generate the probability distribution of Fig. 7,which is more suitable than that of Fig. 5. In Fig. 7, the range predicted from the elevation map differs from the range sensor data because the elevation map gives an environment different from the real environment. The probability calculated by the modified sensor model, p_2, however, is larger than p_1 calculated by (6). The probabilities of the samples close to the true robot pose, therefore, would remain relatively high, and it might prevent those samples from being easily eliminated in the resampling steps of MCL.

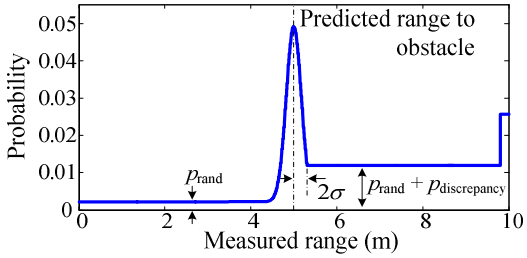

Fig. 6. Modified sensor model for probability calculation based on difference between sensor data and predicted range data.

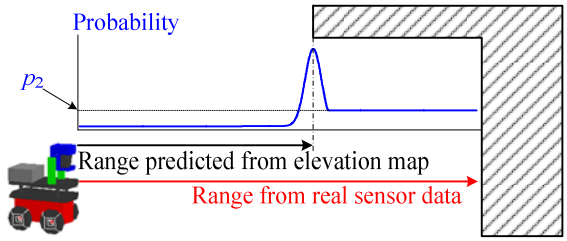

Fig. 7. Probability distribution by modified sensor model with elevation map.

VI. Experimental Results

MCL was implemented on a standard notebook and evaluated using real sensor data obtained from a mobile robot, Pioneer 3AT equipped with a SICK LMS291 laser scanner, as shown in Fig. 8. The laser scanner was tilted by a DC motor and its tilt angle was read by an encoder. During localization, the laser scanner was fixed horizontally. The absolute roll and pitch angles of the robot were sensed by the inertial measurement unit (IMU), and the yaw angle and motion increments were sensed by both the wheel encoder and IMU. Combining these data allowed the estimation of 6 DOF motion in the global coordinate frame [25]. Since the absolute roll and pitch angles were sensed by IMU, four states, (x, y, z, yaw), of the robot pose were estimated by MCL. Figure 9 shows the environment for the experiments and the reference elevation map which was given in advance.

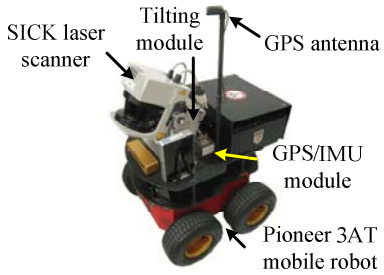

Fig. 8. Robot used for research.

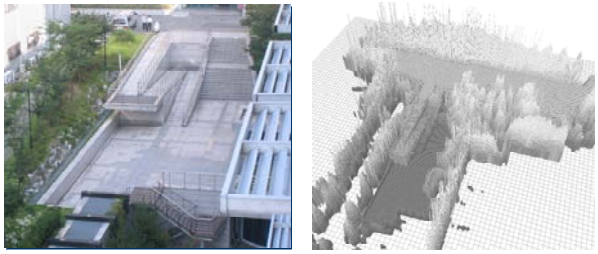

Fig. 9. Environment and reference elevation map.

Figure 10 shows the difference between sample convergences with the conventional and modified sensor models during global localization. The samples whose predicted range data were similar to the real sensor data had high probabilities, and the globally distributed samples converged to one small region after several iterations of MCL. Figure 10(a) shows the experimental environment. The robot predicted the range to an obstacle, $d_{\text{prediction}}$, from A of the elevation map. The real range, d_{sensor}, was measured from B by a laser scanner. These two ranges, however, were different from each other in this case. In Fig. 10(b), the discrepancy between the map and the environment could not be considered by the conventional sensor model. Therefore, the samples based on which $d_{\text{prediction}}$ was predicted to be similar to d_{sensor} had high probabilities, and they finally tended to converge to the incorrect pose. On the other hand, in Fig. 10(c), the probabilities of samples were calculated by the modified sensor model. The samples based on which $d_{\text{prediction}}$ was predicted to be different from d_{sensor} also had high probability as well as the samples based on which $d_{\text{prediction}}$ was predicted to be similar to d_{sensor} because other portions of data which were predicted and sensed not from A and B corresponded to each other. And the samples finally tended to converge to the correct pose, despite the discrepancy between the elevation map and the environment.

Figure 11 shows the success rates of global localization by the conventional sensor model and the modified sensor model. A robot pose is not known and many samples are initially distributed on the entire free space. In this research, localization was assumed successful if all samples came within 1 m to the true robot pose in 15 resampling steps of MCL. The success rate of MCL in the outdoor environment with the conventional sensor model was lower than 40% because of the discrepancy between the elevation map and the environment. Similar results were reported in [3]. Note that the success rate of MCL with the modified sensor model, which was constructed by simply modifying the conventional sensor model, was 10%-15% higher than that with the conventional sensor model.

Figure 12 shows the localization errors during local tracking. This experiment was carried out with 1,000 samples with the known initial robot pose in the environment of Fig. 9. The length of the travel distance was about 150 m. As shown in Fig. 12, the errors of MCL with the modified sensor model differed little from those with the conventional sensor model. And MCL with the conventional sensor model and MCL with the modified sensor model had the same computational overhead.

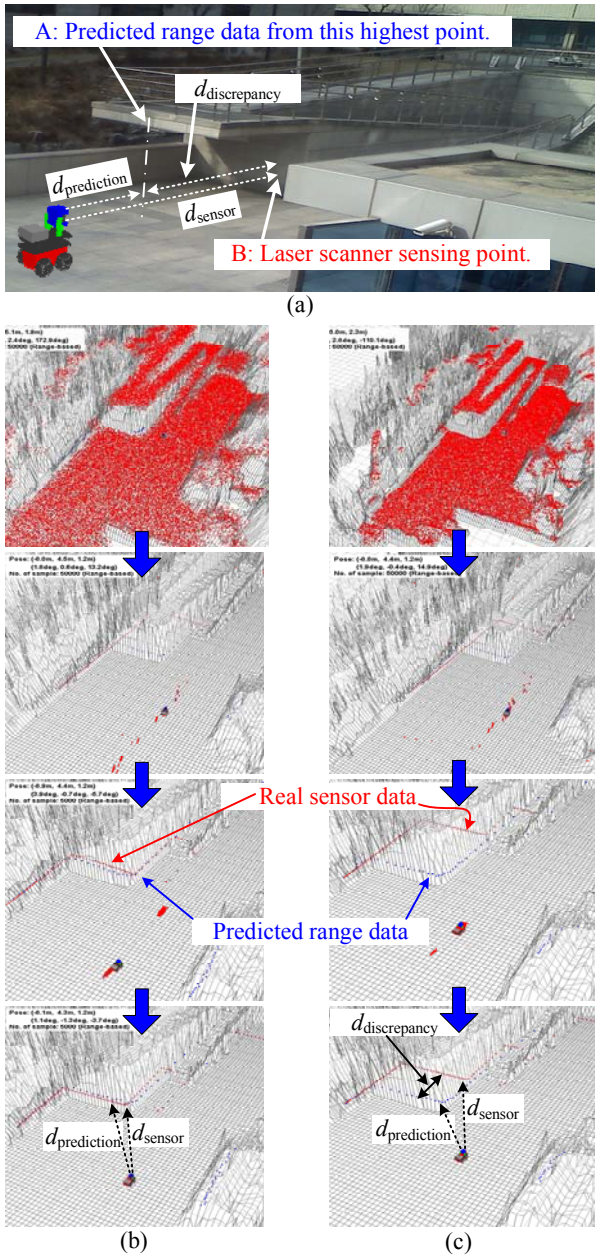

Fig. 10. Sample convergence during global localization; (a) by conventional sensor model, (b) modified sensor model, and (c) experimental environment.

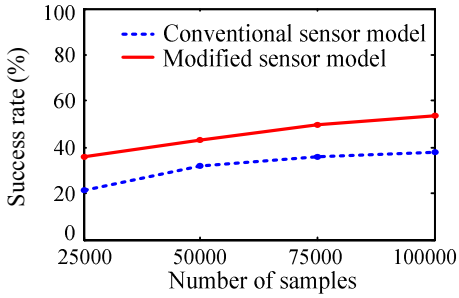

Fig. 11. Success rates of global localization by conventional and modified sensor models, respectively.

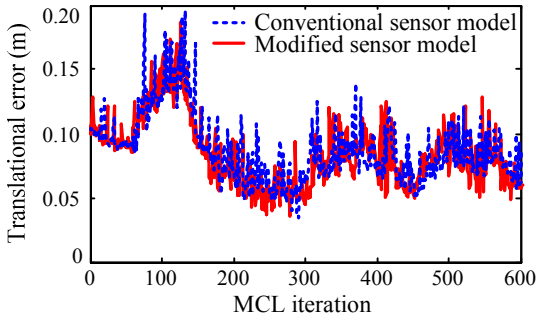

Fig. 12. Localization errors during local tracking with 1,000 samples.

VII. Conclusions

In this paper, the conventional sensor model for MCL was modified to improve the localization performance when an elevation map was used as the main reference map. A new probability distribution to deal with the discrepancy between the elevation map and the real environment was added to the conventional sensor model which consists of three different probability distributions. The local tracking performance of MCL with the modified sensor model was almost identical with that with the conventional sensor model, but the performance of global localization was improved by the proposed sensor model. Furthermore, the use of the modified sensor model instead of the conventional sensor model did not increase the computational cost, and therefore, the proposed sensor model is considered to be very useful for outdoor localization by MCL when an elevation map needs to be used as the main reference map.

References

[1] S. Thrun, "Learning Metric-Topological Maps for Indoor Mobile Robot Navigation," *Artificial Intelligence*, vol. 99, pp. 21-71, Feb., 1998.

[2] H. Choset and K. Nagatani, "Topological Simultaneous Localization and Mapping (SLAM): Toward Exact Localization without Explicit Localization," *IEEE Trans. on Robotics and Automation*, vol. 17, pp. 125-137, Apr., 2001.

[3] R. Kummerle, R. Triebel, P. Pfaff and W. Burgard, "Monte Carlo Localization in Outdoor Terrains Using Multilevel Surface Maps," *Journal of Field Robotics*, vol. 25, pp. 346-359, Jun., 2008.

[4] R. Triebel, P. Pfaff and W. Burgard, "Multi-Level Surface Maps for Outdoor Terrain Mapping and Loop Closing," *Proc. IEEE Int. Conf. Intelligent Robots and Systems*, pp. 2276-2282, Oct., 2006.

[5] C. Parra, R. Murrieta, M. Devy and M. Briot, "3-D Modelling and Robot Localization from Visual and Range Data in Natural Scenes," *Proc. Int. Conf. on Vision Systems*, vol. 1542 in *LNCS*, pp. 450-468, Jan., 1999.

[6] F. Nashashibi, P. Fillatreau, B. Dacre-Wright and T. Simeon, "3-D Autonomous Navigation in a Natural Environment," *Proc. IEEE Int. Conf. Robotics and Automation*, pp. 433-439, May, 1994.

[7] P. Frederick, R. Kania, M. D. Rose, D. Ward, U. Benz, A. Baylot, M. J. Willis and H. Yamauchi, "Spaceborne Path Planning for Unmanned Ground Vehicles (UGVs)," *Proc. IEEE Conf. Military Communications (MILCOM)*, pp. 3134-3141, Oct., 2005.

[8] H. Durrant-Whyte and T. Bailey, "Simultaneous Localization and Mapping: Part I, the essential algorithms," *IEEE Trans. on Robotics and Automation Magazine*, vol. 13, pp. 99-110, Feb., 2006.

[9] L. Yufeng and S. Thrun, "Results for Outdoor-SLAM Using Sparse Extended Information Filters," *Proc. IEEE Int. Conf. Robotics and Automation*, pp. 1227-1233, Sept., 2003.

[10] R. Katz, N. Melkumyan, J. Guivant, T. Bailey, J. Nieto and E. Nebot, "Integrated Sensing Framework for 3D Mapping in Outdoor Navigation," *Proc. IEEE Int. Conf. Intelligent Robots and Systems*, pp. 2264-2269, Oct., 2006.

[11] D. M. Cole and P. M. Newman, "Using Laser Range Data for 3D SLAM in Outdoor Environments," *Proc. IEEE Int. Conf. Robotics and Automation*, pp. 1556-1563, May, 2006.

[12] J. Leonard and H. Durrrant-Whyte, "Mobile robot localization by tracking geometric beacon," *IEEE Transaction on Robotics and Automation*, vol. 7, pp. 376-382, 1991.

[13] D. Fox, W. Burgard and S. Thrun, "Active markov localization for mobile robots," *Robotics and Autonomous Systems*, vol. 25, pp. 195-207, 1998.

[14] F. Dellaert, D. Fox and S. Thrun, "Monte Carlo localization for mobile robots," *Proc. of International Conference on Robotics and Automation*, pp. 1322-1328, 1999.

[15] D. Fox, W. Burgard, F. Dellaert and S. Thrun, "Monte Carlo localization: efficient position estimation for mobile robots," *Proc. of 6th National Conference on Artificial Intelligence*, pp. 343-349, 1999.

[16] J.-S. Gutmann, W. Burgard, D. Fox and K. Konolige, "An experimental comparison of localization methods," *Proc. of IEEE/RSJ International Conference on Intelligent Robots and Systems*, pp. 736-743, 1998.

[17] S. Thrun, W. Burgard and D. Fox, *Probabilistic Robotics*, The MIT Press, Cambridge, 2005.

[18] C. Frueh and A. Zakhor, "Constructing 3D City Models by Merging Ground-based and Airborne Views," *Proc. Conf. Computer Vision and Pattern Recognition*, pp. 562-569, Jun., 2003.

[19] C. Frueh and A. Zakhor, "An Automated Method for Large-Scale Ground-based City Model Acquisition," *Trans. on International Journal of Computer Vision*, vol. 60, pp. 5-24, Jan., 2004.

[20] F. Dellaert, D. Fox and S. Thrun, "Monte Carlo localization for mobile robots," *Proc. of International Conference on Robotics and Automation*, pp. 1322-1328, 1999.

[21] D. Fox, W. Burgard, F. Dellaert and S. Thrun, "Monte Carlo localization: efficient position estimation for mobile robots," *Proc. of 6th National Conference on Artificial Intelligence*, pp. 343-349, 1999.

[22] A. Doucet, S. Godsill and C. Andrieu, "On sequential Monte Carlo sampling methods for Bayesian filtering," *Statics and Computing*, vol. 10, pp. 197-208, 2000.

[23] A. Doucet, N.J. Gordon and J.F.G. de Freditas, *Sequential Monte Carlo methods in practice*, Springer, Berlin, 2001.

[24] D. Fox, *Markov Localization: A Probabilistic Framework for Mobile Robot Localization and Navigation*, Doctoral Thesis, Institute of Computer Science, Univ. of Bonn, Germany, 1998.

[25] S. Lacrois, A. Mallet, D. Bonnafous, G. Bauzil, S. Fleury and M. Herrb, "Autonomous Rover Navigation on Unknown Terrains: Functions and Integration," *Trans on Int. Journal of Robotics Research*, vol. 21, pp. 913-942, Oct., 2002.